

OSLNet: Deep Small-Sample Classification with an Orthogonal Softmax Layer

Xiaoxu Li, Dongliang Chang, Zhanyu Ma, Zheng-Hua Tan, Jing-Hao Xue, Jie Cao, Jingyi Yu, and Jun Guo

Abstract—A deep neural network of multiple nonlinear layers forms a large function space, which can easily lead to overfitting when it encounters small-sample data. To mitigate overfitting in small-sample classification, learning more discriminative features from small-sample data is becoming a new trend. To this end, this paper aims to find a subspace of neural networks that can facilitate a large decision margin. Specifically, we propose the *Orthogonal Softmax Layer* (OSL), which makes the weight vectors in the classification layer remain orthogonal during both the training and test processes. The Rademacher complexity of a network using the OSL is only $\frac{1}{K}$, where K is the number of classes, of that of a network using the fully connected classification layer, leading to a tighter generalization error bound. Experimental results demonstrate that the proposed OSL has better performance than the methods used for comparison on four small-sample benchmark datasets, as well as its applicability to large-sample datasets. Codes are available at: <https://github.com/dongliangchang/OSLNet>.

Index Terms—Deep neural network, Orthogonal softmax layer, Overfitting, Small-sample classification.

I. INTRODUCTION

In recent years, due to the advances of deep learning, large-scale image classification has achieved massive success [1], [2]. However, in many real-world problems, big data are difficult to obtain [3]–[5]. In addition, when human beings learn a concept, millions or billions of data samples are unnecessary [6], [7]. Therefore, small-sample classification [8]–[10] has received much attention recently in the deep learning community [7], [11]–[15]. However, a deep neural network usually models a large function space, which results in overfitting and instability problems that are difficult to avoid in small-sample classification [16]–[18].

Small-sample classification can be roughly classified into two families depending on whether there are unseen categories to be predicted [19]–[21]. In this work, we mainly focus on the one with no unseen category to be predicted. A key challenge in this direction is how to avoid overfitting. Up to now, many methods have been proposed to mitigate overfitting in small-sample classification, such as data augmentation [22]–[24],

X. Li and J. Cao are with School of Computer and Communication, Lanzhou University of Technology, China.

X. Li, D. Chang, Z. Ma and J. Guo are with the Pattern Recognition and Intelligent System Laboratory, School of Artificial Intelligence, Beijing University of Posts and Telecommunications, Beijing, China.

Z.-H. Tan is with the Department of Electronic Systems, Aalborg University, Denmark.

J.-H. Xue is with the Department of Statistical Science, University College London, U.K.

J. Yu is with the School of Information Science and Technology, ShanghaiTech University, China.

domain adaptation [3], [18], regularization [25], ensemble methods [26] and learning discriminative features [27].

Recently, learning discriminative features has become a new trend to improve the classification performance in deep learning. Methods such as the large-margin loss and the virtual softmax method [28] work well on both large-sample and small-sample data. However, these methods either add some constraints on the loss function or make some assumptions on data, which increases the difficulty of optimization and limits the applicable types of data. On the contrary, our goal in this work is to find a subspace of neural networks that can readily obtain a large decision margin and learn highly discriminative features. Specifically, we aim at obtaining a large decision margin through achieving large angles between the weight vectors of different classes in the classification layer (i.e., output layer), in part motivated by the observation that the larger the angles between the weight vectors in the classification layer are, the better the generalization performance is, as shown in Fig. 1.

Therefore, we propose the *Orthogonal Softmax Layer* (OSL) for neural networks as a replacement of the fully connected classification layer. In the proposed OSL, some connections are removed and the weight vectors of different classes are pairwise orthogonal. Due to fewer connections and larger between-class angles, the OSL can mitigate the co-adaptation [29] of a network while enhancing the discrimination ability of features, as we will show in this work. Compared with traditional networks with a fully connected classification layer, a neural network with the OSL has significantly lower model complexity and is ideally suitable for small-sample classification. Experimental results demonstrate that the proposed OSL performs better on four small-sample benchmark datasets than the methods used for comparison as well as its applicability to large-sample datasets.

A number of methods have been proposed to maintain the orthogonality of the weight vectors during the training process of networks [30]–[36]. These methods maintain the orthogonality of weight vectors either for reducing gradients vanishing and obtaining a stable feature distribution [30], [31], [33] or for generating decorrelated feature representation [32], [37]. Unlike these methods, our work does not constrain the optimization process to obtain an orthogonal weight matrix, but constructs a network structure with a fixed orthogonal classification layer by removing some connections so that it can mitigate the co-adaptation between the parameters. The main contributions of this paper are threefold:

- 1) A novel layer, namely the Orthogonal Softmax Layer (OSL), is proposed. The OSL is an alternative to the

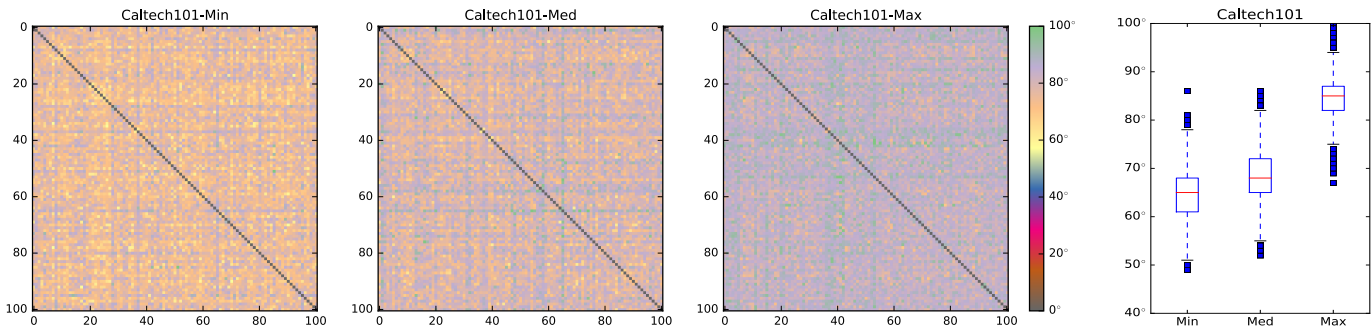


Fig. 1. The first three matrices show the final angles of the weight vectors from the classification layer in the fully connected network (FC). We ran 60 rounds of simulations on the Caltech101 dataset, see Section IV for more details. The results are selected from the minimum (Caltech101-Min), median (Caltech101-Med) and maximum (Caltech101-Max) of 60 sets of accuracies. The corresponding accuracies are 88.07%, 89.28% and 90.35%, respectively. The boxplot shows the off-diagonal angles of these three matrices.

fully connected classification layer and can be used as the classification layer (i.e., the output layer) of any neural network for classification.

- 2) The proposed OSL can reduce the difficulty of network optimization due to militating the co-adaptation between the parameters in the classification layer.
- 3) A network with the proposed OSL can have a lower generalization error bound than a network with a fully connected classification layer.

II. RELATED WORK

Data augmentation. Data augmentation, which artificially inflates the training set with label preserving transformations, is well-suited to limited training data [38], [39], such as the methods of deformation [40], [41], generating more training samples [42], and pseudo-label [43]. However, data augmentation is computationally costly to implement [23].

Domain adaptation. The goal of domain adaptation [44], [45] is to use a model, which is trained in the source domain with a sufficient amount of annotated training data while trained in the target domain with little or no training data [46]–[49]. The simplest approach to domain adaptation is to use the available annotated data in the target domain to fine-tune a convolutional neural network (CNN) pre-trained on the source data, such as ImageNet [48], [50]–[52], which is a commonly used method for small-sample classification [53]. However, as both the initial learning rate and the optimization strategy of neural networks affect the final performance, this kind of methods is difficult to avoid the overfitting problem in small-sample classification. In addition, the knowledge distillation [54], a kind of method for knowledge transfer, compresses the knowledge in an ensemble into a single model. Overall, this type of methods have some limitations: the original domain and the target domain cannot be far away from each other, and overfitting of neural networks on small-sample data remains difficult to avoid.

Learning discriminative features. There are several recent studies that explicitly encourage the learning of discriminative features and enlarge the decision margin, such as the virtual softmax [28], the L-softmax loss [27], the A-softmax loss [55], the GM loss [56], and the center loss [57]. The virtual softmax

enhances the discrimination ability of learned features by injecting a dynamic virtual negative class into the original softmax, and it indeed encourages the features to be more compact and separable across the classes [28]. The L-softmax loss and the A-softmax loss are built on the cross-entropy loss. They introduce new classification scores to enlarge the decision margin. However, the two losses increase the difficulty of network optimization. The GM loss assumes that the deep features of sample points follow a Gaussian mixture distribution. It still has some limitations since many real data are not well suitable to be modelled by Gaussian mixture distributions. The center loss [57] developed a regularization term for the softmax loss function, that is, features of the samples from the same class must be close in the Euclidean distance. In addition to the loss functions above, other loss functions either consider the imbalance of data [58] or the noisy labels in the training data [59]. The focal loss [58] places different weights on different training samples: the samples that are difficult to be identified will be assigned a large weight. The truncated L_q loss [59], a noise-robust loss function, can overcome noisy labels in the training data. Unlike these studies for improving the loss function, our method obtains discriminative features by constructing a fixed orthogonal classification layer by removing some connections.

Ensemble methods. The ensemble methods [60]–[64] have been shown to be effective to address the overfitting problem. The SnapShot ensembling [26] only trains one time and obtains multiple base classifiers for free. This method leverages the nonconvex nature of neural networks and the ability of the stochastic gradient descent (SGD) to converge to or escape from local minima on demand. It finds multiple local minima of loss, saves the weights of the corresponding base networks, and combines the predictions of the corresponding base networks. The temporal ensembling, a parallel work to the SnapShot ensembling, can be trained on a single network. The predictions made on different epochs correspond to an ensemble prediction of multiple subnetworks due to dropout regularization [63]. Both the SnapShot ensembling and the temporal ensembling work well on small-sample data. However, generally speaking, using an entire ensemble of models to make prediction is cumbersome and computationally costly.

Regularization. The L_2 regularization method [65] is often applied to mitigate overfitting in neural networks. Dropout [66] mitigates overfitting mainly by randomly dropping some units (with their connections) from the neural network during training, which prevents the units from coadapting too much. DropConnect [67] is a variant of Dropout, where each connection can be dropped with probability p . Both approaches introduce dynamic sparsity within the model. The fully connected layer with DropConnect becomes a sparsely connected layer, where the connections are randomly selected during the training stage. In addition, the orthogonality regularization is also a kind of regularization techniques that are able to stabilize the distribution of activation over layers within CNNs and improve the performance of CNNs [37], [68].

In addition to these methods, there exist implicit regularization techniques, such as batch normalization and its variants [69], [70]. Batch normalization (BN) [71] aims to normalize the distribution of the layer input of neural networks, hence it can reduce the internal covariate shift in the training process. Built on BN, the decorrelated batch normalization (DBN) [69] decorrelates the layer input and improved BN on CNNs. Iterative normalization (IterNorm) [70] further improves DBN towards efficient whitening and iteratively normalizes the data along the eigenvectors in the training process. Both DBN and IterNorm adjust the distribution of samples so that features of samples are pairwise orthogonal. Unlike them, the proposed OSL forces the weights in the classification layer to be pairwise orthogonal (Please refer to Fig. 2 for details.) The orthogonality in OSL is to assign the input neurons to different output neurons so that it can mitigate the co-adaptation between the parameters.

III. THE ORTHOGONAL SOFTMAX LAYER

Dropping some connections in the neural networks are adopted by Dropout and DropConnect, as well as the proposed OSL. To make the proposed OSL easy to understand, we first review Dropout and DropConnect.

A. Preliminaries

We denote the input vector and the output vector of a layer in the neural network as $\mathbf{v} = [v_1, v_2, \dots, v_D]^T$ and $\mathbf{r} = [r_1, r_2, \dots, r_K]^T$, respectively, and denote the activation function as a . Following the formulation in [67], the fully connected layer is defined as $\mathbf{r} = a(\mathbf{W}\mathbf{v})$ with weight matrix \mathbf{W} .

Based on the above denotations, the fully connected layer with Dropout is defined as $\mathbf{r} = \mathbf{m} \star a(\mathbf{W}\mathbf{v})$, where \star represents element wise product, \mathbf{m} is a K -dimension binary vector. The j th element of \mathbf{m} , $m_j \sim \text{Bernoulli}(1-p)$, $j \in \{1, 2, \dots, K\}$ and p is probability for dropping a neuron. Moreover, the fully connected layer with DropConnect is defined as $\mathbf{r} = a((\mathbf{M} \star \mathbf{W})\mathbf{v})$, where \star represents element wise product and each entry of binary matrix \mathbf{M} is $M_{ij} \sim \text{Bernoulli}(1-q)$, $i \in \{1, 2, \dots, D\}$ and $j \in \{1, 2, \dots, K\}$, and q is the probability for dropping a connection.

B. Mathematical Interpretation of the OSL

To maintain large angles among the weights in the classification layer, we drop some connections in the fully connected classification layer, make the weights in the classification layer be pairwise orthogonal and propose the *Orthogonal Softmax Layer (OSL)*, see Fig. 2). The OSL is defined as

$$\mathbf{r} = \text{softmax}((\mathbf{M} \star \mathbf{W})\mathbf{v}), \quad (1)$$

where \star represents element wise product, and \mathbf{M} , the mask matrix of \mathbf{W} , is a fixed and predesigned block diagonal matrix as

$$\mathbf{M} = \begin{bmatrix} M_{1,1} & 0_{1,2} & \cdots & 0_{1,K} \\ 0_{2,1} & M_{2,2} & \cdots & 0_{2,K} \\ \vdots & \vdots & \ddots & \vdots \\ 0_{K,1} & 0_{K,2} & \cdots & M_{K,K} \end{bmatrix}, \quad (2)$$

where K is the number of classes, M_{ij} is a column vector whose elements are 1, and 0_{ij} is a zero column vector where every element is 0. The matrix is fixed during the training and test phases. If we consider $\mathbf{M} \star \mathbf{W}$ as one matrix, the column vectors are pairwise orthogonal, which is equivalent to introducing a strong prior that the angles between the weights of different categories are all 90° .

C. Remarks for OSL

Here are some remarks on the OSL. First, the OSL is an alternative to the classification layer (i.e., the last fully connected layer) of a neural network. In contrast, the Dropconnect cannot be effectively used in the classification layer, because if all the connections of a output neuron are dropped, the neural network or part of it cannot be trained.

Second, a neural network with the OSL is a single model throughout the training and test processes, since it first drops some connections and subsequently fixes the structure in both the training and test phases. This is in contrast with the DropConnect method. DropConnect randomly drops connections with a given probability during the training phase, but no connection is dropped in the test phase. DropConnect can be considered an implicit ensemble method.

Third, in the OSL, different neurons of the last hidden layer connect to different output neurons. This setup assigns each hidden neuron to one and only one specific class that they are responsible prior to the start of training, so the difficulty level of training the neural network is reduced. Moreover, the solution space of a network with the OSL is a subset of the solution space of its corresponding network with a fully connected classification layer, which implies low model complexity of the former.

D. Implementation of the OSLNet

The OSL can be used in any type of networks for classification, such as the fully connected network or CNN. For convenience, we call a neural network with the OSL as *OSLNet*. The OSLNet uses the OSL as the classification layer instead of a fully connected classification layer, and the structure of the other layers are kept the same as a standard network, e.g., a neural network with the fully connected classification layer.

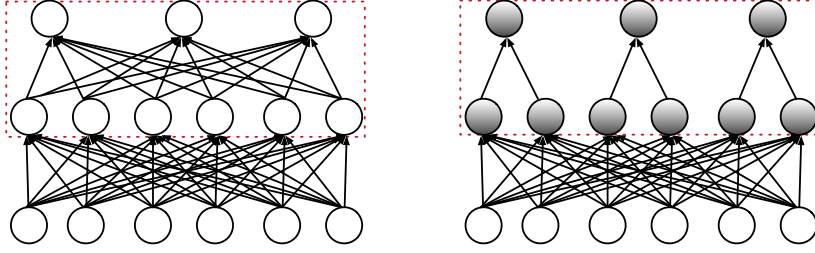


Fig. 2. The left-hand panel is a standard network with the fully connected classification layer, and the right-hand panel is a network with the Orthogonal Softmax Layer (OSL, indicated by shadow).

Different from the implementation of the fully connected classification layer, the forward computation of the OSL needs to conduct the dot product (see (1)) between the predesigned matrix \mathbf{M} (see (2)) and weights matrix \mathbf{W} .

E. The Generalization Error Bound of the OSLNet

In this section, we discuss the generalization error bound of the OSLNet in terms of the Rademacher complexity [72], [73]. We define the entire network into two parts: the classification layer and the layers of extracting features. The classification layer refers to the last fully connected layer in a neural network, and the layers of extracting features refer to all layers except the classification layer. Based on the definitions, a standard network with the fully connected classification layer can be represented as $f(x; \mathbf{W}_s, \mathbf{W}_g)$ and the OSLNet can be represented as $f(x; \mathbf{M} \star \mathbf{W}_s, \mathbf{W}_g)$, where \mathbf{W}_s and $\mathbf{M} \star \mathbf{W}_s$ are the parameters of the classification layer for the two networks, respectively, and \mathbf{W}_g are the parameters of the layers for extracting features.

Lemma 1. (Network Layer Bound [67]) Let \mathcal{G} denote the class of D -dimensional real functions $\mathcal{G} = [\mathcal{Q}_j]_{j=1}^D$, and \mathcal{H} denote a linear transform function $\mathcal{H} : R^D \rightarrow R$, which is parametrized by \mathbf{W} with $\|\mathbf{W}\|_2 \leq B$; then $\hat{R}_l(\mathcal{H} \circ \mathcal{G})$, the empirical Rademacher complexity of $(\mathcal{H} \circ \mathcal{G})$, satisfies $\hat{R}_l(\mathcal{H} \circ \mathcal{G}) \leq \sqrt{DB} \hat{R}_l(\mathcal{Q})$.

Theorem 2. (Complexity of *OSLNet*). Following the notation in Lemma 1, we further let $\hat{R}_l(\mathcal{O})$ denote the empirical Rademacher complexity of an OSLNet. If the weights of the OSL meet $|\mathbf{W}_s| \leq B_s$, we will have $\hat{R}_l(\mathcal{O}) \leq (\frac{D}{\sqrt{k}} B_s) \hat{R}_l(\mathcal{Q})$.

Proof. First, we denote the empirical Rademacher complexity of a standard network with the fully connected classification layer as $\hat{R}_l(\mathcal{O}_0) = \hat{R}_l(\mathcal{H}_0 \circ \mathcal{G})$. Since no connection has been removed in a standard network with the fully connected classification layer, \mathcal{H}_0 is a linear transform function $\mathcal{H}_0 : R^D \rightarrow R$ and is parametrized by \mathbf{W}_s with $|\mathbf{W}_s| \leq B_s$. Because $|\mathbf{W}_s| \leq B_s$ and the size of \mathbf{W}_s is $D \times K$, we have $\|\mathbf{W}_s\|_2 \leq \sqrt{DK} B_s$. Thus, based on Lemma 1, we can obtain $\hat{R}_l(\mathcal{O}_0) \leq (D\sqrt{K} B_s) \hat{R}_l(\mathcal{Q})$.

Similarly, for OSLNet, we have $\hat{R}_l(\mathcal{O}) = \hat{R}_l(\mathcal{H} \circ \mathcal{G})$. Because in the OSLNet some connections are removed and the weight vectors of different classes are pairwise orthogonal, \mathcal{H} becomes a linear transform function $\mathcal{H} : R^{\frac{D}{k}} \rightarrow R$ and is

parametrized by $\mathbf{M} \star \mathbf{W}_s$ ($\|\mathbf{M} \star \mathbf{W}_s\|_2 \leq \sqrt{D} B_s$). Therefore, based on Lemma 1, we have $\hat{R}_l(\mathcal{O}) \leq (\frac{D}{\sqrt{k}} B_s) \hat{R}_l(\mathcal{Q})$. \square

The analysis above shows that the bound of empirical Rademacher complexity for the OSLNet is only $\frac{1}{K}$ of that for a standard network. In addition, the empirical error of the OSLNet is close to the standard model in terms of accuracy and cross-entropy loss on the training data, as shown in Fig. 6. Therefore, according to the relationship between a model generalization error bound and an empirical Rademacher complexity (Theorem 3.1 in [72]), the OSLNet has a lower model generalization error bound than the standard network.

IV. EXPERIMENTAL EVALUATION

To evaluate the performance of the proposed OSL, we compare OSLNet with other methods on four small-sample datasets and three large-sample datasets. These evaluation serve four purposes:

- 1) To compare the proposed OSL with state-of-the-art methods on small-sample image classification (Sec. IV-C, Sec. IV-D, and Sec. IV-E);
- 2) To investigate the effect of modifying the width or depth of the hidden layers on OSLNet (Sec. IV-F and Sec. IV-G), and the effect of changing the feature extractor on OSLNet (Sec. IV-H);
- 3) To demonstrate the discriminability of the features learned from OSLNet (Sec. IV-I);
- 4) To demonstrate the performance of OSL on large-sample image classification (Sec. IV-J).

A. Small-Sample Datasets

For experiments on small-sample image classification, we selected the following four small-sample datasets:

- UIUC-Sports dataset (UIUC)¹ [74]: This dataset contains 8 classes of sports scene images. The total number of images is 1579. The numbers of images for different classes are: bocce (137), polo (182), rowing (250), sailing (190), snowboarding (190), rock climbing (194), croquet (236), and badminton (200).
- 15Scenes [75]: This dataset contains 15 classes of natural scene images: coast, forest, highway, inside city, mountain, open country, street and tall building. We randomly

¹<http://vision.stanford.edu/lijiayi/Resources.html>

TABLE I

COMPARISON OF THE CLASSIFICATION PERFORMANCE ON THE *UIUC-Sports* (UIUC), *15Scenes*, a subset of *80-AI* (80-AI), AND *Caltech101* DATASETS. THE METHODS ARE: *Fully connected network* (FC), *Focal loss* (FOCAL), *Center loss* (CENTER), *Truncated L_q loss* (T- L_q), *Iterative Normalization* (ITERNORM), *Decorrelated Batch Normalization* (DBN), *Dropout*, *Large-Margin Softmax Loss* (LSOFTMAX), *SnapShot Ensembling* (SNAPSHOT), AND THE *proposed OSL* (OS), AND *SnapShot Ensembling of OS* (OS-SNAPSHOT). EACH METHOD HAS BEEN EVALUATED FOR 60 ROUNDS.

Datasets	Measure	FC	Focal	Center	T- L_q	IterNorm	DBN	Dropout	Lsoftmax	SnapShot	OS	OS-SnapShot
UIUC	Mean	0.8837	0.8787	0.8347	0.8573	0.8506	0.8378	0.8889	0.8946	0.8950	0.9016	0.9041
	Std.	0.0151	0.0135	0.0283	0.1693	0.0242	0.0752	0.0113	0.0076	0.0175	0.0055	0.0030
15Scenes	Mean	0.8331	0.8285	0.7911	0.6551	0.8291	0.8005	0.8321	0.8434	0.8413	0.8439	0.8464
	Std.	0.0080	0.0066	0.0152	0.3319	0.0067	0.0358	0.0101	0.0054	0.0066	0.0037	0.0022
80-AI	Mean	0.5316	0.5291	0.4678	-	0.5828	0.4552	0.5445	0.3886	0.5825	0.6157	0.6192
	Std.	0.0139	0.0159	0.0356	-	0.0074	0.0291	0.0305	0.0413	0.0091	0.0031	0.0025
Caltech101	Mean	0.8927	0.8881	0.8644	-	0.8814	0.9254	0.8865	0.9168	0.9290	0.9127	0.9369
	Std.	0.0046	0.0047	0.0062	-	0.0068	0.0028	0.0077	0.0071	0.0020	0.0044	0.0011

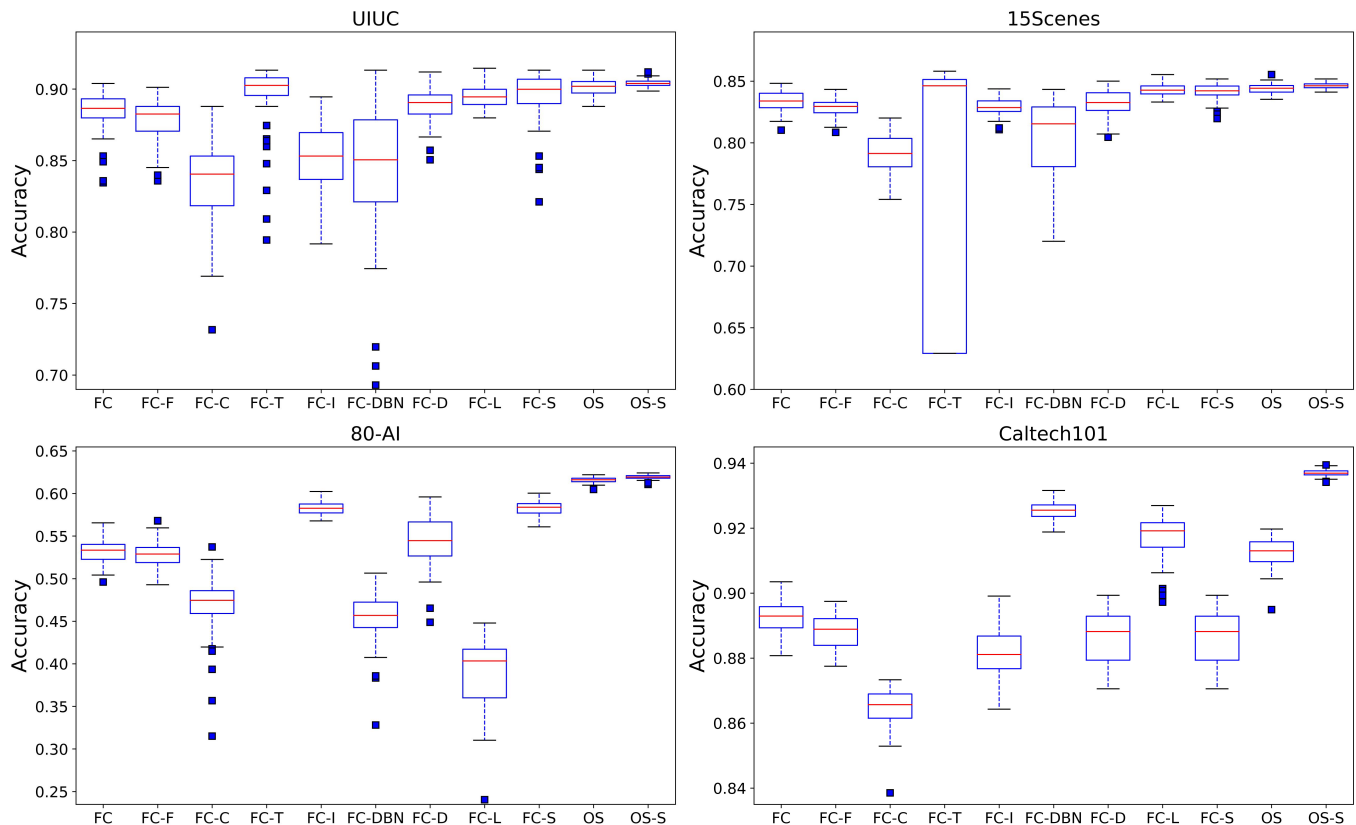


Fig. 3. Comparison of the accuracies obtained by FC, Focal (FC-F), Center (FC-C), T- L_q (FC-T), IterNorm (FC-I), DBN (FC-DBN), Dropout (FC-D), Lsoftmax (FC-L), SnapShot (FC-S), OS, and OS-SnapShot (OS-S), via boxplots on the UIUC, 15Scenes, 80-AI, and Caltech101 datasets. The central mark is the median, and the edges of the box are the 25th and 75th percentiles. The outliers are individually marked. In the boxplots, each method has been evaluated for 60 rounds.

select 200 images for each class, so the total number of images is 3000.

- Subset of the Scenes dataset on AI Challenger (80-AI): This dataset contains 80000 images in 80 classes of daily scenes, such as airport terminal and amusement park. The size of the classes is 600-1000². We randomly select 200 images for each class, so the total number of images is 16000.
- Caltech101 [76]: This dataset contains pictures of objects in 101 categories, and the size of each category is approx-

imately 40-800 images. The total number of pictures in the dataset is 4000.

For the 15Scenes and 80-AI datasets, in both the training and test datasets, each class contains 100 samples. For the UIUC and Caltech101 datasets, unlike the 15Scenes and 80-AI datasets, different classes have different number of samples, and we randomly split the data of each class into the training and test sets evenly.

We adopted a CNN feature extractor, VGG16 [77], which was pre-trained on ImageNet. First, we resized the images into identical sizes of 256×256 and directly extracted the

²<https://challenger.ai/competition/scene/subject>

TABLE II
COMPARISON OF CLASSIFICATION ACCURACIES ON THE UIUC, 15SCENES, 80-AI AND CALTECH101 DATASETS WHEN THE TRAINING DATA ARE REDUCED. THE NOTATION DATASETNAME- n DENOTES THE CONFIGURATION WHERE THE TRAINING DATA IN THE NAMED DATASET IS REDUCED BY n DATA POINTS FOR EVERY CLASS FROM THE ORIGINAL TRAINING SETS, WHEREAS THE TEST SETS REMAIN UNCHANGED. EACH METHOD RUNS 60 ROUNDS ON EACH DATASET.

Datasets	Measure	FC	Dropout	Lsoftmax	SnapShot	OS	OS-SnapShot
UIUC-20	Mean	0.8715	0.8776	0.8800	0.8822	0.8891	0.8894
	Std.	0.0134	0.0146	0.0082	0.0129	0.0074	0.0080
UIUC-30	Mean	0.8577	0.8631	0.8682	0.8682	0.8793	0.8692
	Std.	0.0135	0.0145	0.0087	0.0142	0.0060	0.0118
UIUC-40	Mean	0.8447	0.8493	0.8563	0.8585	0.8695	0.8570
	Std.	0.0152	0.0141	0.0086	0.0127	0.0082	0.0145
UIUC-50	Mean	0.8296	0.8349	0.8372	0.8353	0.8461	0.8329
	Std.	0.0115	0.0139	0.0092	0.0174	0.0065	0.0223
Datasets	Measure	FC	Dropout	Lsoftmax	SnapShot	OS	OS-SnapShot
15Scenes-20	Mean	0.8283	0.8209	0.8399	0.8371	0.8401	0.8438
	Std.	0.0067	0.0174	0.0070	0.0077	0.0039	0.0022
15Scenes-40	Mean	0.8181	0.8112	0.8312	0.8299	0.8296	0.8347
	Std.	0.0091	0.0126	0.0066	0.0067	0.0039	0.0026
15Scenes-60	Mean	0.804	0.7965	0.8156	0.8101	0.8129	0.8164
	Std.	0.0090	0.0120	0.0077	0.0066	0.0042	0.0028
15Scenes-80	Mean	0.7781	0.7746	0.7936	0.7837	0.7906	0.7979
	Std.	0.0084	0.0220	0.0070	0.0078	0.0049	0.0066
Datasets	Measure	FC	Dropout	Lsoftmax	SnapShot	OS	OS-SnapShot
80-AI-20	Mean	0.5169	0.5241	0.4116	0.5693	0.5999	0.6023
	Std.	0.0141	0.0401	0.0217	0.0076	0.0027	0.0040
80-AI-40	Mean	0.4977	0.5019	0.4016	0.5475	0.5772	0.5680
	Std.	0.0202	0.0282	0.0240	0.0080	0.0031	0.0118
80-AI-60	Mean	0.4766	0.4605	0.4022	0.5099	0.5386	0.5089
	Std.	0.0121	0.0252	0.0412	0.0086	0.0046	0.0219
80-AI-80	Mean	0.4112	0.4018	0.4043	0.4247	0.4624	0.3696
	Std.	0.0134	0.0210	0.0168	0.0090	0.0118	0.0513
Datasets	Measure	FC	Dropout	Lsoftmax	SnapShot	OS	OS-SnapShot
Caltech101-5	Mean	0.8774	0.8760	0.9057	0.9163	0.9013	0.9261
	Std.	0.0048	0.0088	0.0059	0.0028	0.0050	0.0013
Caltech101-10	Mean	0.8583	0.8579	0.8856	0.8976	0.8867	0.9037
	Std.	0.0047	0.0079	0.0071	0.0035	0.0056	0.0015

image features using the VGG16 network. Finally, we kept the features of the last convolutional layer and simply flattened them. The feature dimension of each image is $512 \times 8 \times 8 = 32768$.

B. The Compared Methods and Their Implementation

To evaluate the classification performance of the proposed OSL, we compare the following methods: 1) fully connected network (FC); 2) Focal loss (Focal) [58]; 3) Center loss (Center) [57]; 4) Truncated L_q loss (T- L_q) [59]; 5) Iterative normalization (IterNorm) [70]; 6) Decorrelated batch normalization (DBN) [69]; 7) Dropout; 8) large-margin softmax loss (Lsoftmax) [27]; 9) SnapShot ensembling of FC (SnapShot) [26]; 10) the proposed OSL (OS); and 11) SnapShot ensembling of OS (OS-SnapShot).

For FC, we used a fully connected network with two layers, where the activation functions of the first and second layers are rectified linear unit function (*Relu*) and *Softmax*, respectively. FC is optimized by minimizing the softmax cross-entropy loss based on the minibatch gradient descent. The optimization algorithm is the RMSprop with the initial learning rate 0.001, the batch size is 32, and the number of epochs is 100.

For DBN and IterNorm, we placed them before each linear layer of FC. For DBN, we set group-number = 2 for the UIUC

and 15 scenes datasets and set group-number = 16 for the 80-AI and Caltech101 datasets. For IterNorm, we set $T = 10$ and group-number = 8 for all the four datasets.

For Focal, Center, T- L_q , and Lsoftmax, we adopted the focal loss [27], center loss, truncated L_q loss, and large-margin softmax loss [27] to replace the softmax cross-entropy loss used in FC, respectively. For these four loss functions, we tried multiple sets of parameter values and selected the setting with best performance. Specifically, for Focal, we selected $\gamma = 0.5$ for the 80-AI dataset and $\gamma = 0.3$ for other three datasets. For Center, we selected a small loss weight, $\lambda = 1e - 10$. For T- L_q , we set $q = 0.5$ and $k = 0.1$ for the UIUC dataset, and $q = 0.1$ and $k = 0.1$ for the 15Scenes dataset. However, on the 80-AI and Caltech101 datasets, we did not find a set of q and k that makes T- L_q fit the training data. For Lsoftmax, we set $m = 2$. Other settings were kept the same as those for FC.

For Dropout, we added a Dropout layer after the hidden layer of FC. The probability that a neuron unit should be dropped is 0.5. Other settings of Dropout are identical to FC.

The SnapShot here is a SnapShot ensembling built on the FC network, where the learning rate is learned by using a cyclic cosine annealing method [78], and the number of SnapShots is 2. For OS, we replaced the fully connected classification layer with the proposed OSL in FC and other settings were identical to that of FC. For OS-SnapShot, except

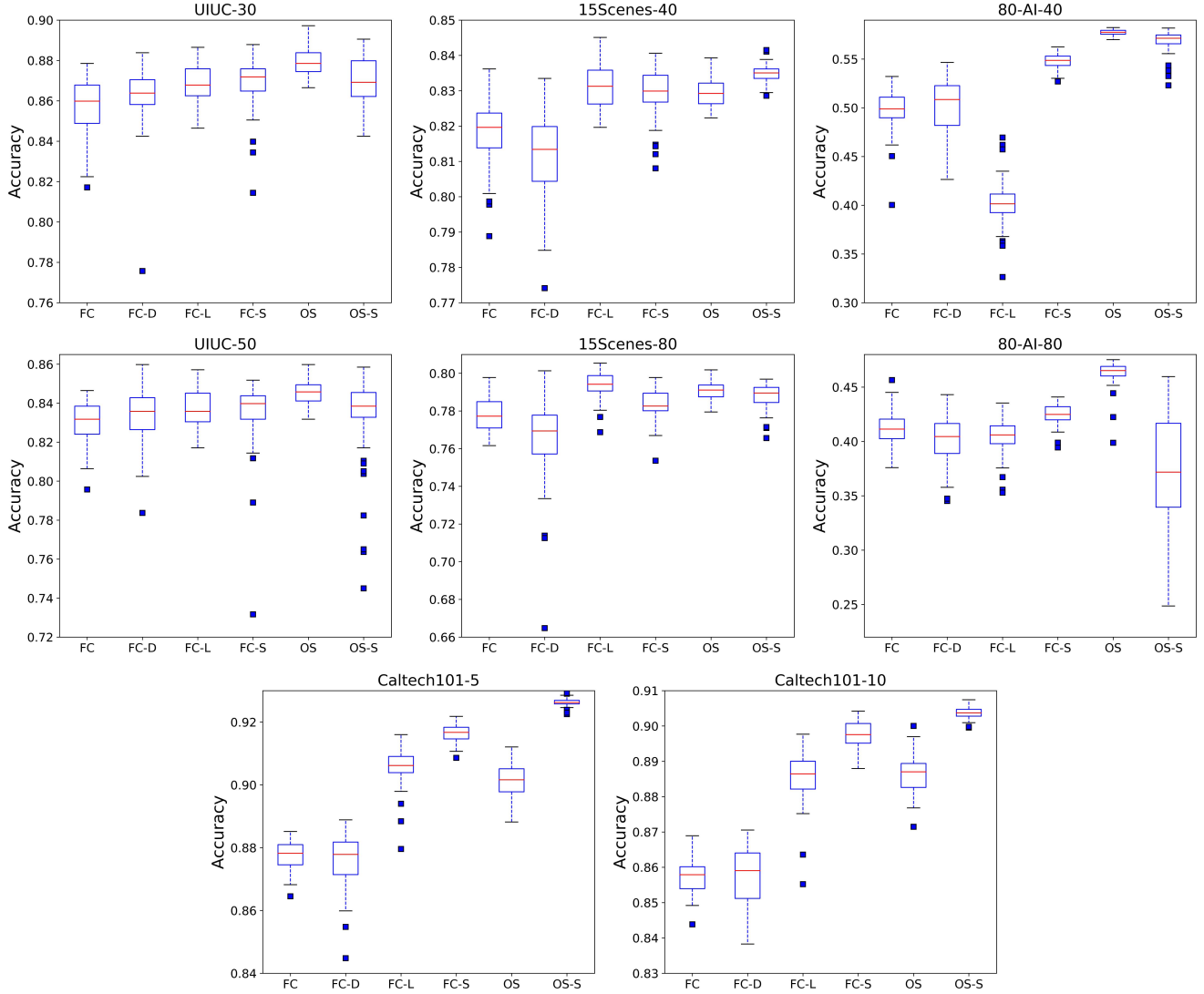


Fig. 4. Comparison of accuracies obtained by FC, Dropout (FC-D), Lsoftmax (FC-L), SnapShot (FC-S), OS and OS-SnapShot (OS-S) via boxplots on the UIUC-30, UIUC-50, 15Scenes-40, 15Scenes-80, 80-AI-40, 80-AI-80, Caltech101-5 and Caltech101-10 datasets. In the boxplots, each method runs 60 rounds.

for the structure of base network, other settings are identical to that of SnapShot.

All the methods have been implemented with PyTorch [79].

C. Classification Accuracy

We ran FC, Focal, Center, $T-L_q$, IterNorm, DBN, Dropout, Lsoftmax, SnapShot, OS and OS-SnapShot on the UIUC, 15Scenes, 80-AI and Caltech101 datasets for 60 rounds each. The mean and the standard deviation of the classification accuracy are listed in Table I, and the boxplot of classification accuracy is shown in Fig. 3. Larger mean and smaller standard deviation indicate better performance.

Table I shows that, on the four datasets, FC is easy to overfit and has unstable performance. Moreover, Focal, Center, and $T-L_q$ underperform FC. IterNorm outperforms FC on 80-AI and DNB performs better than FC on Caltech101, and in other cases IterNorm and DBN underperform FC. Dropout performs slightly better than FC on UIUC, competitively with FC on 80-AI, and worse than FC on 15Scenes and Caltech101. Lsoftmax

performs better than FC on UIUC, 15Scenes and Caltech101 but slightly worse than FC on 80-AI. SnapShot always has better performance than FC on the four datasets. OS performs better than FC, Dropout and Lsoftmax on UIUC, 15Scenes and 80-AI, showing larger mean and smaller variance. OS performs better than FC and Dropout, but worse than Lsoftmax and SnapShot, on Caltech101. We also evaluated the SnapShot ensembling version of OS, denoted as OS-SnapShot, and it obtains better performance on all the four datasets.

Fig. 3 demonstrates that on the UIUC-Sports dataset, the boxplot of OS is more compact than those of FC, Focal, Center, $T-L_q$, IterNorm, DBN, Dropout, Lsoftmax and SnapShot. Moreover, it has no bad-performing outlier. On the 15Scenes dataset, the boxplot of OS is more compact than those of FC, Dropout and SnapShot, but is close to that of Lsoftmax. On the 80-AI dataset, the boxplot of OS is also more compact than those of other methods, and both the central mark and the edges of the box are higher than those of other methods used for comparison. On the Caltech101 dataset, the boxplot

TABLE III

THE p -VALUES OF THE PROPOSED METHOD (OS) AND THE REFERRED METHODS, FC, DROPOUT, LSOFTMAX AND SNAPSHOT, BY THE PAIRED STUDENT’S T-TEST. EACH METHOD RUNS 60 ROUNDS ON EACH DATASET.

Datasets	FC	Dropout	Lsoftmax	SnapShot
UIUC	< 0.005	< 0.005	< 0.005	0.0116
UIUC-20	< 0.005	< 0.005	< 0.005	< 0.005
UIUC-30	< 0.005	< 0.005	< 0.005	< 0.005
UIUC-40	< 0.005	< 0.005	< 0.005	< 0.005
UIUC-50	< 0.005	< 0.005	< 0.005	< 0.005
15S.	< 0.005	< 0.005	0.6014	0.0087
15S.-10	< 0.005	< 0.005	0.8284	0.0057
15S.-30	< 0.005	< 0.005	0.1437	0.7747
15S.-50	< 0.005	< 0.005	0.0225	0.0090
15S.-70	< 0.005	< 0.005	0.0093	< 0.005
80-AI	< 0.005	< 0.005	< 0.005	< 0.005
80-AI-10	< 0.005	< 0.005	< 0.005	< 0.005
80-AI-30	< 0.005	< 0.005	< 0.005	< 0.005
80-AI-50	< 0.005	< 0.005	< 0.005	< 0.005
80-AI-70	< 0.005	< 0.005	< 0.005	< 0.005
Cat.101	< 0.005	< 0.005	< 0.005	< 0.005
Cat.101-5	< 0.005	< 0.005	< 0.005	< 0.005
Cat.101-10	< 0.005	< 0.005	< 0.005	< 0.005

TABLE IV

CLASSIFICATION ACCURACIES OBTAINED BY FC AND OS ON THE UIUC AND 15SCENES (15Sce.) DATASETS WHEN WE CHANGE THE SIZE OF THE HIDDEN LAYER. FC AND OS HAVE 2 LAYERS AND THE SIZE OF THEIR HIDDEN LAYER IS SHOWN. EACH SETTING OF FC AND OS HAS BEEN EVALUATED FOR 60 ROUNDS.

UIUC	16	32	64	128	256	512
FC-Mean	0.8525	0.8837	0.8949	0.8800	0.8973	0.8945
FC-Std.	0.0218	0.0151	0.0146	0.0074	0.0073	0.0096
OS-Mean	0.9002	0.9016	0.9022	0.8987	0.8877	0.8836
OS-Std.	0.0074	0.0054	0.0056	0.0055	0.0070	0.0065
15Sce.	16	32	64	128	256	512
FC-Mean	N/A	0.8070	0.8331	0.8409	0.8415	0.8431
FC-Std.	N/A	0.0131	0.0080	0.0062	0.0059	0.0061
OS-Mean	N/A	0.8419	0.8439	0.8429	0.8401	0.8373
OS-Std.	N/A	0.0043	0.0037	0.0038	0.0036	0.0040

of OS is also more compact and higher than those of FC and Dropout, but is lower than those of Lsoftmax and SnapShot. Finally, the boxplots of OS-SnapShot is always more compact than those of all other compared methods, with both the central mark and the edges of the boxes higher.

D. Classification Accuracy for Different Training Set Sizes

Table II and Fig. 4 show that, on the UIUC datasets with decreased training set sizes, Dropout shows small improvement over FC. Lsoftmax achieves larger mean and lower variance than FC and Dropout. SnapShot, an ensemble method, obtains larger mean, but the variance is similar to the others. It is encouraging to see that OS has larger mean and lower standard deviation than all the four compared methods on all the different sizes of training sets. OS-SnapShot outperforms OS in terms of the mean accuracy.

On the 15Scenes dataset, Dropout performs worse than FC, in terms of variance and mean. Lsoftmax consistently performs better than FC. SnapShot shows slight improvement but is worse than Lsoftmax. OS still performs well, as expected. OS-SnapShot improves the mean compared with OS.

On the 80-AI dataset, Lsoftmax and Dropout perform worse than FC. Lsoftmax notably is difficult to converge with the four training sizes. SnapShot performs better than FC, Dropout and Lsoftmax. OS has smaller variances and larger means and performs much better than all other methods.

On the Caltech101 dataset, SnapShot performs better than FC, Dropout and Lsoftmax. OS has smaller variances and larger means than FC and Dropout and has similar performance to Lsoftmax. OS-SnapShot performs the best.

In summary, the proposed OSL performs better than other compared methods on these datasets.

E. Paired Student’s t-test

The experimental results presented in the previous sections show that the proposed OSL obtains better performance. To confirm that the improvement is statistically significant, we performed a paired Student’s t-test [80] for OS vs. FC, OS vs. Dropout, OS vs. Lsoftmax, and OS vs. SnapShot, and the p -values are listed in Table III. Following [81], we set the significance level as 0.05.

For the tests of OS vs. FC, all the p -values are much smaller than the significance level. Thus, the null hypothesis that FC and OS have the identical mean is always rejected. Likewise, the null hypothesis that Dropout has the identical mean to OS is also rejected.

In terms of Lsoftmax, on the UIUC, 80-AI and Caltech101 datasets, the null hypothesis that Dropout and OS have the identical mean is always rejected. However, on the 15Scenes dataset, the p -values are larger than the significance level in most cases. Thus, on 15Scenes, the null hypothesis that Lsoftmax and OS have the identical mean is generally not rejected.

For SnapShot, on the 80-AI and Caltech101 datasets, the null hypothesis that SnapShot and OS have the identical mean is always rejected. However, on the UIUC and 15Scenes datasets, the null hypothesis that SnapShot has the identical mean with OS is not always rejected.

F. Effect of Changing the Width of the Hidden Layers on OSLNet

In the previous experiments, our method and all the baseline methods used the network structure with 32 neurons in the last hidden layer. To explore the effect of the width of the hidden layer on the performance of OSLNet, we changed the number of hidden neurons in both FC and OS from 16 to 512 on the UIUC dataset, with other settings unchanged. At the same time, we also changed the number of the hidden neurons from 32 to 512 on the 15Scenes dataset, with other settings unchanged. FC and OS were evaluated on the two datasets for 60 rounds, respectively.

From Table IV, we can observe that, with the increase in the width of network, the mean of FC has generally slight improvement on UIUC, and the standard deviation decreases. That is, FC generally performs better when the number of the hidden neurons is increased. In contrast, OS performs better when the number of the hidden neurons is small. Particularly, when the number of the hidden neurons is 16, OS is much

TABLE V

COMPARISON OF THE CLASSIFICATION ACCURACIES ON THE UIUC AND 15SCENES DATASETS WHEN WE VARY THE DEPTH OF THE NEURAL NETWORKS. THE SIZES OF THE HIDDEN LAYERS ARE LISTED. EACH STRUCTURE OF FC AND OS IS TESTED FOR 60 ROUNDS; THE MEAN AND STANDARD DEVIATION (STD.) ARE LISTED IN THE CELLS OF THE TABLE.

UIUC	Measure	32-8	64-32-8	128-64-32-8	256-128-64-32-8	512-256-128-64-32-8
FC	Mean	0.8837	0.8834	0.8796	0.8687	0.8545
	Std.	0.0151	0.0101	0.0096	0.0101	0.0129
OS	Mean	0.90167	0.8933	0.8872	0.8575	0.8482
	Std.	0.0055	0.0089	0.0095	0.0136	0.0169
15Scenes	Measure	64-15	128-64-15	256-128-64-15	512-256-128-64-15	
FC	Mean		0.8331	0.8378	0.8391	0.8288
	Std.		0.0080	0.0061	0.0056	0.0077
OS	Mean		0.8439	0.8406	0.8404	0.8208
	Std.		0.0037	0.0062	0.0057	0.0083

TABLE VI

COMPARISON OF THE CLASSIFICATION PERFORMANCE ON THE UIUC AND 15SCENES DATASETS, WITH 60 ROUNDS OF VALUATIONS FOR EACH METHOD.

UIUC	Measure	FC	Focal	Center	IterNorm	DBN	Dropout	SnapShot	OS	OS-SnapShot
VGG16	Mean	0.8787	0.8347	0.8506	0.8378	0.8837	0.8889	0.8950	0.9016	0.9041
	Std.	0.0151	0.0135	0.0283	0.0242	0.0752	0.0113	0.0175	0.0054	0.0030
DenseNet121	Mean	0.5532	0.5389	0.3248	0.3163	0.5234	0.4697	0.6225	0.6438	0.6954
	Std.	0.0631	0.0797	0.1105	0.0560	0.1197	0.0891	0.0391	0.0633	0.0158
15Scenes	Measure	FC	Focal	Center	IterNorm	DBN	Dropout	SnapShot	OS	OS-SnapShot
VGG16	Mean	0.8331	0.8285	0.7911	0.8291	0.8005	0.8321	0.8413	0.8439	0.8464
	Std.	0.0080	0.0007	0.0152	0.0007	0.0357	0.0110	0.0066	0.0037	0.0022
DenseNet121	Mean	0.5783	0.5653	0.3497	0.4836	0.5694	0.5443	0.6366	0.6200	0.6799
	Std.	0.0465	0.0490	0.1029	0.1158	0.0546	0.0379	0.0154	0.0359	0.0045

superior to FC. Moreover, on 15Scenes, a similar pattern can be observed. In addition, OS has better performances when approximately 2 to 4 hidden neurons are assigned to each class on these two datasets with 8 and 15 classes, respectively.

G. Effect of Changing the Depth of the Hidden Layers on OSLNet

We also evaluate the effect of the depth of the network on OSLNet. In particular, we varied the depth of the network from 2 to 5 layers and from 2 to 4 layers in both FC and OS on the UIUC and 15Scenes datasets, respectively. Each structure of FC and OS is evaluated on UIUC and 15Scenes for 60 rounds. The size of each layer, the depth of each layer, the corresponding mean and standard deviation of accuracy are listed in Table V.

From Table V, we can observe that, on UIUC, the mean values of FC and OS become smaller, when the depth is increased, that is, the performance of both FC and OS decreases, and OS decreases faster than FC. A similar pattern is also found on 15Scenes. Therefore, shallow structures of both FC and OS perform better than deep ones of FC and OS on the two datasets.

H. Effect of Changing Feature Extractor on OSLNet

In all the experiments presented above, we used a pre-trained VGG16 as the feature extractor. In this section, we changed the feature extractor to a pre-trained DenseNet121 and ran all the compared methods on the UIUC and 15Scenes datasets for 60 rounds each. The classification results are shown in Table VI. Here, we do not list the performance of

$T-L_q$ and Lsoftmax, as it cannot fit the training data if the feature extractor is DenseNet121.

From Table VI, we can observe that: 1) On the UIUC and 15scenes datasets, each method performs better with the VGG16 feature extractor than with the DenseNet121 feature extractor. 2) When the feature extractor is DenseNet121, on the UIUC dataset, the proposed OS outperforms all the compared methods, and on the 15scenes dataset, OS underperforms SnapShot and outperform other compared methods. Then we can conclude that OS-SnapShot performs best on both datasets.

In summary, the performance comparison on DenseNet121 is similar to those on VGG16, which further shows the applicability of the OSL.

I. Feature Visualization

To gain insights on the proposed OSL, we visualize the input features of OSL. Take the experiments on the UIUC dataset as an example: the input dimension of OSL is 32, and the output dimension of OSL is 8, as determined by the number of classes. Therefore, according to the design of OSL, each output neuron (i.e., each class) is assigned 4 input neurons. For example, the 1st-4th dimensional input features are for the class 0, and the 5th-8th dimensional input features are for the class 1 (The class labels are from 0 to 7 on the UIUC dataset). We use t-SNE [82] to visualize the input features of OSL in Fig. 5. In Fig. 5, the first column is for the 32-dimensional input features without truncation, and the following three columns are for the 4th-8th dimensional features, the 13th-16th dimensional features, the 21th-24th

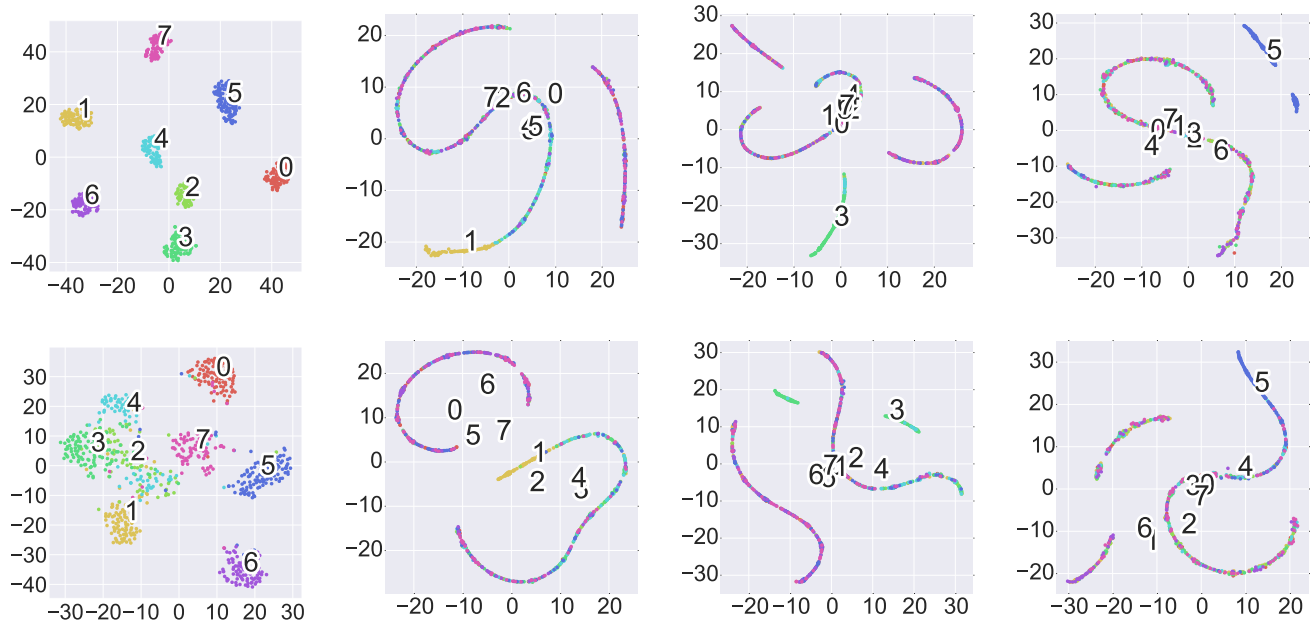


Fig. 5. Visualization of the input feature of the OSL via t-SNE. The four columns from left to right are: 1) the 32-dimensional input feature (without truncation) of OSL, 2) the 4th-8th dimensional features, 3) the 13th-16th dimensional features, and 4) the 21st-24th dimensional features, of which the last three columns correspond to the classes 1, 3 and 5 in the OSL, respectively. Upper row: the training data. Lower row: the test data.

dimensional features, which correspond to the classes 1, 3 and 5 in the OSL, respectively.

From Fig. 5, it can be observed that, in the first column, the samples from different classes are separate. In the following three columns, the samples of the corresponding class are put to one end of a feature curve or a place far from the features of other classes. A similar pattern appears for other classes in the UIUC dataset and in other datasets. This demonstrates that, in the proposed OSL, the input neurons assigned to each class are indeed responsible for learning discriminative features for differentiating that class from other classes.

J. OSLNet on Large-sample Datasets

To evaluate the applicability of our OSL on large-sample classification, we selected the following three datasets.

- **CIFAR-10:** This dataset [83] consists of 60000 32×32 color images in 10 classes with 6000 images per class. There are 50000 training images and 10000 test images. The classes are as follows: airplane, automobile, bird, cat, deer, dog, frog, horse, ship and truck.
- **CIFAR-100:** This dataset [83] consists of 60000 32×32 color images in 100 classes with 600 images per class. There are 500 training images and 100 test images per class.
- **MNIST:** This dataset of handwritten digits [84] has a training set of 60000 examples and a test set of 10000 examples. It is a subset of a larger set available from MNIST. The digits have been size-normalized and centered in a fixed-size image. The size of the images is 28×28 .

We compare the following methods: 1) CNN; 2) SnapShot ensembling of CNN (CNN-SnapShot); 3) a CNN with OSL (OS-CNN); and 4) SnapShot ensembling of OS-CNN (OS-CNN-SnapShot). The classification results are listed in Table VII and demonstrated in Fig. 6.

On the CIFAR-10 and CIFAR-100 datasets, for CNN, we used the VGG16 style network, where the convolutional layer has batch normalization, and the fully connected parts have 2 hidden layers of 16 units each. The epoch number is 400, and the learning rate decreases from 0.01 to 0 by using the cosine annealed method. The optimization method is SGD. For OS-CNN, we only replaced the last fully connected layer with the OS layer in CNN, while other settings unchanged. For CNN-SnapShot, the learning rate decreases from 0.01 to 0 by using the annealed cosine method within 200 epochs, which restarted to the identical process one more time. The total number of epochs is 400, and the number of SnapShot networks is 2. Other settings are identical to those for CNN. For OS-CNN-SnapShot, except for the classification layer, other settings are identical to that for CNN-SnapShot.

On the MNIST dataset, we followed the CNN structure published by PyTorch for MNIST. In the structure, there are two modules including convolution (Maxpooling and Relu activation) and two fully connected layers with 50 hidden neurons. The optimization method remains to be SGD, and the learning rate decreases from 0.01 to 0 as the cosine annealed method is used. The epoch number is 400. For OS-CNN, CNN-SnapShot and OS-CNN-SnapShot, except for the structure of CNN, other settings were the same as that for the CIFAR-10 and CIFAR-100 datasets.

From the classification accuracy shown in Table VII, the curves of the cross-entropy loss, and the accuracy shown in

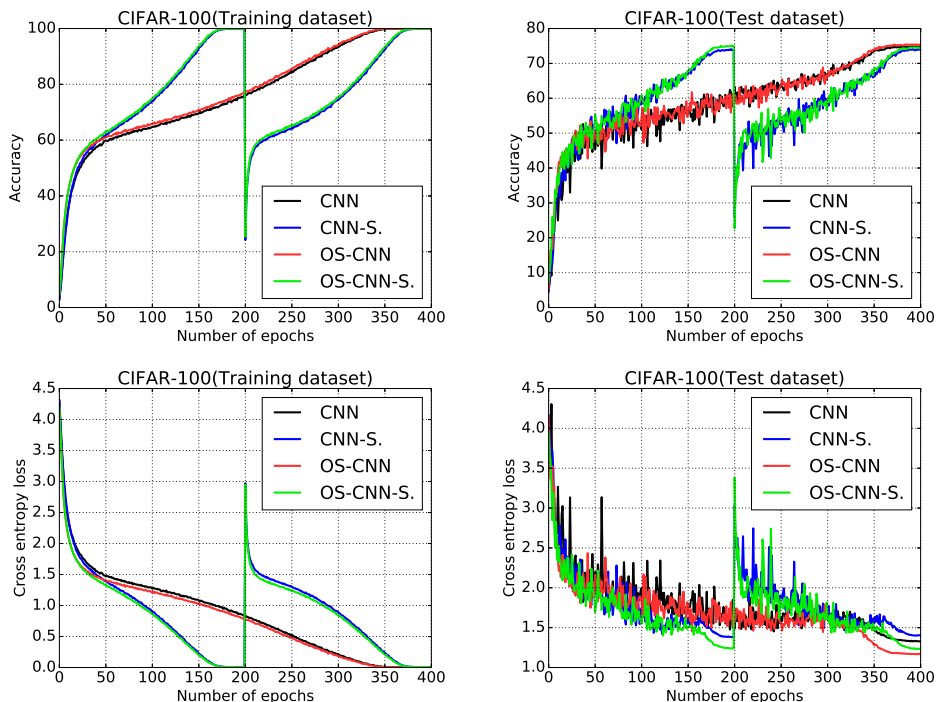


Fig. 6. The cross-entropy loss and accuracy of CNN, CNN-SnapShot (CNN-S.), OS-CNN, and OS-CNN-SnapShot (OS-CNN-S.) on the CIFAR-100 dataset. The left-hand column is for the training data, and the right-hand column is for the test data.

TABLE VII
COMPARISON OF CLASSIFICATION ACCURACY OF CNN, CNN-SNAPSHOT ENSEMBLING (CNN-S.), CNN WITH OSL (OS-CNN) AND OS-CNN-SNAPSHOT ENSEMBLING (OS-CNN-S.).

Datasets	CNN	CNN-S.	OS-CNN	OS-CNN-S.
CIFAR-10	0.9379	0.9445	0.9418	0.9468
CIFAR-100	0.7467	0.7648	0.7529	0.7690
MNIST	0.9921	0.9928	0.9925	0.9926

Fig. 6, it can be observed that CNN and OS-CNN have similar performance on the three datasets. That is, the proposed OSL is also applicable for large-sample classification.

K. Discussion

The focal loss places large weights on the samples that are difficult to identify; the center loss constructs a constraints that the features of samples from the same class must be close in the Euclidean distance; and the truncated L_q loss is a noise-robust loss. In the experiments above, the three loss functions are not effective on the four small-sample datasets. It can also be observed that IterNorm and DBN perform unstably, which may be because, while accelerating optimization of neural networks, they do not have any particular mechanism to improve the classification performance of networks.

Among all the compared methods in the experiments on small-samples datasets, Dropout is an implicit ensemble method: in the training process it trains many subnetworks of the original network, and in the test phase no neuron is dropped. On the four small-sample datasets, Dropout do

not show remarkable advantages over the network without dropouts.

Lsoftmax introduces a large margin into the cross-entropy softmax loss function to learn more discriminative features. The key problem of this method is that it is not easy to converge. Thus, it does not perform well in some experiments with a reduced training size. In contrast, the proposed OSL method converges easily.

The Snapshot is a strong baseline among the compared methods and obtains relatively larger mean values and relatively smaller variances. However, although the method is trained only once in the training process and combines the predictions of all Snapshot networks in the test phase, due to the correlation of the base networks, the Snapshot increases the performance of FC slightly.

The proposed method on small-samples datasets shows higher accuracy and better stability, which are mainly attributed to the OSL, where some connections are removed and the angles among the weights of different classes are maintained as 90° from the beginning to the end during training. Having large angles among the weights of different classes in the classification layer is an important precondition to obtain a decision rule with a large margin, when the L_2 norms of the weights are not considered. In addition, which class each neuron of the last hidden layer should serve exclusively is determined prior to the start of training, so the difficulty of training can be significantly reduced. The experimental results of changing the width and depth of the network suggest that when a thin and shallow structure is selected, the OSL can obtain a better performance. In addition, experimental results

of our OSL on the three large-sample image datasets show that, although developed for small-sample classification, OSL can also be well applied to large-sample classification.

Even though OSL has demonstrated superior performance, it has its own limitations. For example, due to the design of OSL, the number of neurons of the last hidden layer should be larger than the class number. Therefore, when the class number is large, *e.g.*, 1000, a large number of neurons will be required, which will increase the flexibility of network. We leave it as an open problem for the future.

V. CONCLUSIONS

In this paper, we proposed a new classification layer called *Orthogonal Softmax Layer* (OSL). A network with OSL (OSLNet) has two advantages, *i.e.*, easy optimization and low Rademacher complexity. The Rademacher complexity of OSLNet is $\frac{1}{K}$, where K is the number of classes, of that of a network with the fully connected classification layer. Experimental results on four small-sample datasets provide the following observations for an OSLNet in small-sample classification: 1) It is able to obtain higher accuracy with larger mean and smaller variance than those of the baselines used for comparison. 2) It is statistically significantly better than the baselines. 3) It is more suitable for thin and shallow networks than a fully connected network. Further experiments on three large-sample datasets show that, compared with a CNN with the fully connected classification layer, a CNN with the OSL has a competitive performance for both training and test data.

REFERENCES

- [1] Y. LeCun, Y. Bengio, and G. Hinton, "Deep learning," *Nature*, vol. 521, no. 7553, p. 436, 2015.
- [2] C. Szegedy, W. Liu, Y. Jia, P. Sermanet, S. Reed, D. Anguelov, D. Erhan, V. Vanhoucke, and A. Rabinovich, "Going deeper with convolutions," in *Proceedings of the IEEE Conference on Computer Vision and Pattern Recognition*, 2015, pp. 1–9.
- [3] L. Bruzzone and M. Marconcini, "Domain adaptation problems: A dasvm classification technique and a circular validation strategy," *IEEE Transactions on Pattern Analysis and Machine Intelligence*, vol. 32, no. 5, pp. 770–787, 2010.
- [4] X. Dong, L. Zheng, F. Ma, Y. Yang, and D. Meng, "Few-example object detection with model communication," *IEEE transactions on pattern analysis and machine intelligence*, vol. 41, no. 7, pp. 1641–1654, 2018.
- [5] J. Snell, K. Swersky, and R. Zemel, "Prototypical networks for few-shot learning," in *Advances in Neural Information Processing Systems*, 2017, pp. 4077–4087.
- [6] L. Fei-Fei, R. Fergus, and P. Perona, "One-shot learning of object categories," *IEEE Transactions on Pattern Analysis and Machine Intelligence*, vol. 28, no. 4, pp. 594–611, 2006.
- [7] O. Vinyals and et al., "Matching networks for one shot learning," in *Advances in Neural Information Processing Systems*, 2016, pp. 3630–3638.
- [8] J. Shu, Z. Xu, and D. Meng, "Small sample learning in big data era," *arXiv preprint arXiv:1808.04572*, 2018.
- [9] C. Zhang, C. Li, and J. Cheng, "Few-shot visual classification using image pairs with binary transformation," *IEEE Transactions on Circuits and Systems for Video Technology*, 2019.
- [10] H. Jiang, R. Wang, S. Shan, and X. Chen, "Learning class prototypes via structure alignment for zero-shot recognition," in *Proceedings of the European conference on computer vision (ECCV)*, 2018, pp. 118–134.
- [11] Y. Fu, T. M. Hospedales, T. Xiang, and S. Gong, "Transductive multi-view zero-shot learning," *IEEE Transactions on Pattern Analysis and Machine Intelligence*, vol. 37, no. 11, pp. 2332–2345, 2015.
- [12] A. Santoro, S. Bartunov, M. Botvinick, D. Wierstra, and T. Lillicrap, "One-shot learning with memory-augmented neural networks," *arXiv preprint arXiv:1605.06065*, 2016.
- [13] H. Lu, C. Shen, Z. Cao, Y. Xiao, and A. van den Hengel, "An embarrassingly simple approach to visual domain adaptation," *IEEE Transactions on Image Processing*, vol. 27, no. 7, pp. 3403–3417, 2018.
- [14] J. Choi, J. Krishnamurthy, A. Kembhavi, and A. Farhadi, "Structured set matching networks for one-shot part labeling," in *Proceedings of the IEEE Conference on Computer Vision and Pattern Recognition*, 2018, pp. 3627–3636.
- [15] Z. Fu, T. Xiang, E. Kodirov, and S. Gong, "Zero-shot learning on semantic class prototype graph," *IEEE Transactions on Pattern Analysis and Machine Intelligence*, vol. 40, no. 8, pp. 2009–2022, 2018.
- [16] X. Glorot and Y. Bengio, "Understanding the difficulty of training deep feedforward neural networks," in *Proceedings of the Thirteenth International Conference on Artificial Intelligence and Statistics*, 2010, pp. 249–256.
- [17] C. Zhang, S. Bengio, M. Hardt, B. Recht, and O. Vinyals, "Understanding deep learning requires rethinking generalization," in *International Conference on Learning Representations*, 2016.
- [18] N. Courty, R. Flamary, D. Tuia, and A. Rakotomamonjy, "Optimal transport for domain adaptation," *IEEE Transactions on Pattern Analysis and Machine Intelligence*, vol. 39, no. 9, pp. 1853–1865, 2017.
- [19] W.-Y. Chen, Y.-C. Liu, Y.-C. F. W. Wang, and J.-B. Huang, "A closer look at few-shot classification," in *International Conference on Learning Representations*, 2019.
- [20] Q. Sun, Y. Liu, T.-S. Chua, and B. Schiele, "Meta-transfer learning for few-shot learning," in *Proceedings of the IEEE Conference on Computer Vision and Pattern Recognition*, 2019, pp. 403–412.
- [21] X.-S. Wei, P. Wang, L. Liu, C. Shen, and J. Wu, "Piecewise classifier mappings: Learning fine-grained learners for novel categories with few examples," *IEEE Transactions on Image Processing*, vol. 28, no. 12, pp. 6116–6125, 2019.
- [22] S. Kim, D. Min, S. Kim, and K. Sohn, "Feature augmentation for learning confidence measure in stereo matching," *IEEE Transactions on Image Processing*, vol. 26, no. 12, pp. 6019–6033, 2017.
- [23] L. Perez and J. Wang, "The effectiveness of data augmentation in image classification using deep learning," *arXiv preprint arXiv:1712.04621*, 2017.
- [24] Z. Zhong, L. Zheng, Z. Zheng, S. Li, and Y. Yang, "Camstyle: A novel data augmentation method for person re-identification," *IEEE Transactions on Image Processing*, vol. 28, no. 3, pp. 1176–1190, 2018.
- [25] N. Srivastava, G. E. Hinton, A. Krizhevsky, I. Sutskever, and R. Salakhutdinov, "Dropout: a simple way to prevent neural networks from overfitting," *Journal of Machine Learning Research*, vol. 15, no. 1, pp. 1929–1958, 2014.
- [26] G. Huang, Y. Li, G. Pleiss, Z. Liu, J. E. Hopcroft, and K. Q. Weinberger, "Snapshot ensembles: Train 1, get m for free," in *International Conference on Learning Representations*, 2017.
- [27] W. Liu, Y. Wen, Z. Yu, and M. Yang, "Large-margin softmax loss for convolutional neural networks," in *Proceedings of International Conference on Machine Learning*, 2016, pp. 507–516.
- [28] B. Chen, W. Deng, and H. Shen, "Virtual class enhanced discriminative embedding learning," in *Advances in Neural Information Processing Systems*, 2018, pp. 1946–1956.
- [29] G. E. Hinton, N. Srivastava, A. Krizhevsky, I. Sutskever, and R. R. Salakhutdinov, "Improving neural networks by preventing co-adaptation of feature detectors," *arXiv preprint arXiv:1207.0580*, 2012.
- [30] M. Arjovsky, A. Shah, and Y. Bengio, "Unitary evolution recurrent neural networks," in *International Conference on Machine Learning*, 2016, pp. 1120–1128.
- [31] L. Huang, X. Liu, B. Lang, A. W. Yu, Y. Wang, and B. Li, "Orthogonal weight normalization: Solution to optimization over multiple dependent stiefel manifolds in deep neural networks," in *Thirty-Second AAAI Conference on Artificial Intelligence*, 2018.
- [32] Y. Sun, L. Zheng, W. Deng, and S. Wang, "Svdnet for pedestrian retrieval," in *Proceedings of the IEEE International Conference on Computer Vision*, 2017, pp. 3800–3808.
- [33] D. Xie, J. Xiong, and S. Pu, "All you need is beyond a good init: Exploring better solution for training extremely deep convolutional neural networks with orthonormality and modulation," in *Proceedings of the IEEE Conference on Computer Vision and Pattern Recognition*, 2017, pp. 6176–6185.
- [34] W. Liu, Y.-M. Zhang, X. Li, Z. Yu, B. Dai, T. Zhao, and L. Song, "Deep hyperspherical learning," in *Advances in neural information processing systems*, 2017, pp. 3950–3960.
- [35] W. Liu, R. Lin, Z. Liu, L. Liu, Z. Yu, B. Dai, and L. Song, "Learning towards minimum hyperspherical energy," in *Advances in neural information processing systems*, 2018, pp. 6222–6233.

- [36] P. Mettes, E. van der Pol, and C. Snoek, "Hyperspherical prototype networks," in *Advances in Neural Information Processing Systems*, 2019, pp. 1485–1495.
- [37] P. Rodríguez, J. Gonzalez, G. Cucurull, J. M. Gonfau, and X. Roca, "Regularizing cnns with locally constrained decorrelations," in *International Conference on Learning Representations*, 2017.
- [38] E. D. Cubuk, B. Zoph, D. Mane, V. Vasudevan, and Q. V. Le, "Autoaugmentation: Learning augmentation strategies from data," in *Proceedings of the IEEE Conference on Computer Vision and Pattern Recognition*, 2019, pp. 113–123.
- [39] R. Volpi, H. Namkoong, O. Sener, J. C. Duchi, V. Murino, and S. Savarese, "Generalizing to unseen domains via adversarial data augmentation," in *Advances in Neural Information Processing Systems*, 2018, pp. 5334–5344.
- [40] T. D. Kulkarni, W. F. Whitney, P. Kohli, and J. Tenenbaum, "Deep convolutional inverse graphics network," in *Advances in neural information processing systems*, 2015, pp. 2539–2547.
- [41] A. J. Ratner, H. Ehrenberg, Z. Hussain, J. Dunnmon, and C. Ré, "Learning to compose domain-specific transformations for data augmentation," in *Advances in neural information processing systems*, 2017, pp. 3236–3246.
- [42] A. Shrivastava, T. Pfister, O. Tuzel, J. Susskind, W. Wang, and R. Webb, "Learning from simulated and unsupervised images through adversarial training," in *Proceedings of the IEEE conference on computer vision and pattern recognition*, 2017, pp. 2107–2116.
- [43] A. J. Ratner, C. M. De Sa, S. Wu, D. Selsam, and C. Ré, "Data programming: Creating large training sets, quickly," in *Advances in neural information processing systems*, 2016, pp. 3567–3575.
- [44] M. Wang and W. Deng, "Deep visual domain adaptation: A survey," *Neurocomputing*, vol. 312, pp. 135–153, 2018.
- [45] S. W. Yoon, J. Seo, and J. Moon, "Tapnet: Neural network augmented with task-adaptive projection for few-shot learning," in *International Conference on Machine Learning*, 2019, pp. 7115–7123.
- [46] J. Yosinski, J. Clune, Y. Bengio, and H. Lipson, "How transferable are features in deep neural networks?" in *Advances in neural information processing systems*, 2014, pp. 3320–3328.
- [47] M. Elhoseiny, A. Elgammal, and B. Saleh, "Write a classifier: Predicting visual classifiers from unstructured text," *IEEE Transactions on Pattern Analysis and Machine Intelligence*, vol. 39, no. 12, pp. 2539–2553, 2017.
- [48] E. Tzeng, J. Hoffman, K. Saenko, and T. Darrell, "Adversarial discriminative domain adaptation," in *Proceedings of the IEEE Conference on Computer Vision and Pattern Recognition*, 2017, pp. 7167–7176.
- [49] A. Rozantsev, M. Salzmann, and P. Fua, "Residual parameter transfer for deep domain adaptation," in *Conference on Computer Vision and Pattern Recognition*, no. 4339-4348, 2018.
- [50] S. J. Pan, Q. Yang *et al.*, "A survey on transfer learning," *IEEE Transactions on Knowledge and Data Engineering*, vol. 22, no. 10, pp. 1345–1359, 2010.
- [51] M. Oquab, L. Bottou, I. Laptev, and J. Sivic, "Learning and transferring mid-level image representations using convolutional neural networks," in *Proceedings of the IEEE Conference on Computer Vision and Pattern Recognition*, 2014, pp. 1717–1724.
- [52] M. Long, H. Zhu, J. Wang, and M. I. Jordan, "Deep transfer learning with joint adaptation networks," in *International Conference on Machine Learning*, 2017, pp. 2208–2217.
- [53] W. Ouyang, X. Wang, C. Zhang, and X. Yang, "Factors in finetuning deep model for object detection with long-tail distribution," in *Proceedings of the IEEE conference on computer vision and pattern recognition*, 2016, pp. 864–873.
- [54] G. Hinton, O. Vinyals, and J. Dean, "Distilling the knowledge in a neural network," *arXiv preprint arXiv:1503.02531*, 2015.
- [55] W. Liu, Y. Wen, Z. Yu, M. Li, B. Raj, and L. Song, "Sphereface: Deep hypersphere embedding for face recognition," in *Proceedings of the IEEE conference on computer vision and pattern recognition*, 2017, pp. 212–220.
- [56] W. Wan, Y. Zhong, T. Li, and J. Chen, "Rethinking feature distribution for loss functions in image classification," in *Proceedings of the IEEE Conference on Computer Vision and Pattern Recognition*, 2018, pp. 9117–9126.
- [57] Y. Wen, K. Zhang, Z. Li, and Y. Qiao, "A discriminative feature learning approach for deep face recognition," in *European conference on computer vision*. Springer, 2016, pp. 499–515.
- [58] T.-Y. Lin, P. Goyal, R. Girshick, K. He, and P. Dollár, "Focal loss for dense object detection," in *Proceedings of the IEEE international conference on computer vision*, 2017, pp. 2980–2988.
- [59] Z. Zhang and M. Sabuncu, "Generalized cross entropy loss for training deep neural networks with noisy labels," in *Advances in neural information processing systems*, 2018, pp. 8778–8788.
- [60] P. M. Granitto, P. F. Verdes, and H. A. Ceccatto, "Neural network ensembles: evaluation of aggregation algorithms," *Artificial Intelligence*, vol. 163, no. 2, pp. 139–162, 2005.
- [61] G. Brown and J. L. Wyatt, "The use of the ambiguity decomposition in neural network ensemble learning methods," in *Proceedings of International Conference on Machine Learning*, 2003, pp. 67–74.
- [62] S. Singh, D. Hoiem, and D. Forsyth, "Swapout: Learning an ensemble of deep architectures," in *Advances in Neural Information Processing Systems*, 2016, pp. 28–36.
- [63] S. Laine and T. Aila, "Temporal ensembling for semi-supervised learning," in *International Conference on Learning Representations*, 2017.
- [64] A. Kumar, J. Kim, D. Lyndon, M. Fulham, and D. Feng, "An ensemble of fine-tuned convolutional neural networks for medical image classification," *IEEE Journal of Biomedical and Health Informatics*, vol. 21, no. 1, pp. 31–40, 2017.
- [65] A. Neumaier, "Solving ill-conditioned and singular linear systems: A tutorial on regularization," *SIAM review*, vol. 40, no. 3, pp. 636–666, 1998.
- [66] S. Wager, S. Wang, and P. S. Liang, "Dropout training as adaptive regularization," in *Advances in neural information processing systems*, 2013, pp. 351–359.
- [67] L. Wan, M. Zeiler, S. Zhang, Y. L. Cun, and R. Fergus, "Regularization of neural networks using dropout," in *Proceedings of International Conference on Machine Learning*, 2013, pp. 1058–1066.
- [68] N. Bansal, X. Chen, and Z. Wang, "Can we gain more from orthogonality regularizations in training deep networks?" in *Advances in Neural Information Processing Systems*, 2018, pp. 4261–4271.
- [69] L. Huang, D. Yang, B. Lang, and J. Deng, "Decorrelated batch normalization," in *Proceedings of the IEEE Conference on Computer Vision and Pattern Recognition*, 2018, pp. 791–800.
- [70] L. Huang, Y. Zhou, F. Zhu, L. Liu, and L. Shao, "Iterative normalization: Beyond standardization towards efficient whitening," in *Proceedings of the IEEE Conference on Computer Vision and Pattern Recognition*, 2019, pp. 4874–4883.
- [71] S. Ioffe and C. Szegedy, "Batch normalization: Accelerating deep network training by reducing internal covariate shift," in *International Conference on Machine Learning*, 2015, pp. 448–456.
- [72] M. Mohri, A. Rostamizadeh, and A. Talwalkar, *Foundations of machine learning*. MIT press, 2012.
- [73] P. L. Bartlett and S. Mendelson, "Rademacher and gaussian complexities: Risk bounds and structural results," *Journal of Machine Learning Research*, vol. 3, no. Nov, pp. 463–482, 2002.
- [74] L.-J. Li and L. Fei-Fei, "What, where and who? classifying events by scene and object recognition," in *IEEE International Conference on Computer Vision*. IEEE, 2007, pp. 1–8.
- [75] S. Lazebnik, C. Schmid, and J. Ponce, "Beyond bags of features: Spatial pyramid matching for recognizing natural scene categories," in *Proceedings of the IEEE Conference on Computer Vision and Pattern Recognition*. IEEE, 2006, pp. 2169–2178.
- [76] L. Fei-Fei, R. Fergus, and P. Perona, "Learning generative visual models from few training examples: An incremental bayesian approach tested on 101 object categories," in *Proceedings of the IEEE Conference on Computer Vision and Pattern Recognition Workshops*. IEEE Computer Society, 2004.
- [77] K. Simonyan and A. Zisserman, "Very deep convolutional networks for large-scale image recognition," *arXiv preprint arXiv:1409.1556*, 2014.
- [78] I. Loshchilov and F. Hutter, "Sgdr: Stochastic gradient descent with warm restarts," *arXiv preprint arXiv:1608.03983*, 2016.
- [79] N. Ketkar, "Introduction to pytorch," in *Deep Learning with Python*. Springer, 2017, pp. 195–208.
- [80] D. W. Zimmerman, "Teachers corner: A note on interpretation of the paired-samples t test," *Journal of Educational and Behavioral Statistics*, vol. 22, no. 3, pp. 349–360, 1997.
- [81] D. Singh Chawla, "Big names in statistics want to shake up much-maligned p value," *Nature News*, vol. 548, no. 7665, p. 16, 2017.
- [82] L. v. d. Maaten and G. Hinton, "Visualizing data using t-sne," *Journal of machine learning research*, vol. 9, no. Nov, pp. 2579–2605, 2008.
- [83] A. Krizhevsky and G. Hinton, "Learning multiple layers of features from tiny images," Citeseer, Tech. Rep., 2009.
- [84] Y. LeCun, L. Bottou, Y. Bengio, and P. Haffner, "Gradient-based learning applied to document recognition," *Proceedings of the IEEE*, vol. 86, no. 11, pp. 2278–2324, 1998.